Smart Structures and Systems, *Vol. 24, No. 1 (2019) 141-155*
DOI: https://doi.org/10.12989/sss.2019.24.1.141

Performance analysis of vehicle suspension systems with negative stiffness

Xiang Shi*, Wei Shi and Lanchang Xing

College of Information and Control Engineering, China University of Petroleum (East China), Qingdao, Shandong Province, China

(Received February 28, 2019, Revised March 8, 2019, Accepted March 10, 2019)

Abstract. This work evaluates the influence of negative stiffness on the performances of various vehicle suspension systems, and proposes a re-centering negative stiffness device (NSD). The re-centering NSD consists of a passive magnetic negative stiffness spring and a positioning shaft with a re-centering function. The former produces negative stiffness control forces, and the latter prevents the amplification of static spring deflection. The numerical simulations reveal that negative stiffness can improve the ride comfort of a vehicle without affecting its road holding abilities for either passive or semi-active suspension systems. In general, the improvement degree of ride comfort increases as negative stiffness increases. For passive suspension system, negative stiffness brings in negative stiffness feature in the control forces, which is helpful for the ride comfort of a vehicle. For semi-active suspensions, negative stiffness can alleviate the impact of clipped damping in semi-active dampers, and thus the ride comfort of a vehicle can be improved.

Keywords: negative stiffness, vehicle suspension, passive suspension, semi-active suspension, ride comfort, road holding

1. Introduction

Suspensions are important components of a vehicle. When a vehicle travels on road, suspension systems carry the weight of vehicle body and transmit all forces between the body and the road. Thus, suspension systems are of great importance for the passengers' ride comfort and vehicle's road holding ability, as well as the vehicle's safety and overall performance. Various control technologies have been proposed for vehicle suspension systems, and depending on their operation modes, these technologies can be classified into passive, semi-active and active. Passive vehicle suspensions adopt springs and oil dampers, which have the advantages of design simplicity and cost effectiveness. The design of passive vehicle suspension focuses on optimizing parameters of the suspension systems. However, optimal design performances can only be achieved in a certain frequency range, and is limited for wide frequency range or changed operating conditions (Yao *et al*. 2002, Du *et al*. 2005).

Active suspension systems can produce favorable control forces through actuators. Therefore, excellent performances over a broad range of frequency can be achieved and operating condition changes can be adapted. Various control strategies have been proposed and evaluated for active suspension systems, including linear quadratic regulator (LQR) (Choi *et al*. 1998), H^{∞} control (Karlsson *et al*. 2001), fuzzy logic control (Al-Holou *et al*. 2002), linear parameter-varying and nonlinear backstepping control (Fialho and Balas 2002), skyhook and adaptive neuro active force control (SANAFC) (Priyandoko *et al*. 2009), model-free fractional-order sliding mode control (MFFOSMC) (Wang *et al*. 2018), and contrast-based Fruit Fly Optimization (Kanarachos *et al*. 2018). However, in practice, active suspension system relies on a complicated system that involves sensors, actuators, controllers, external power supplies, and high initial and maintenance costs. Moreover, its performances or even vehicle stability could be adversely affected by measurement noise or power outage.

Semi-active vehicle suspensions can provide better performances than passive suspensions, and their power consumption and cost are much lower than those of active suspensions. As the development of controllable dampers based on magneto-rheological (MR) fluids, semi-active suspensions become more practical in engineering realization (Yao *et al*. 2002) and have drawn the attentions of many researchers. Both theoretical and experimental studies indicate that the performance of semi-active suspension is highly dependent on the algorithm employed (Ying *et al*. 2003, Savaresi, *et al*. 2003, Dong *et al*. 2010). Ahmadian and Vahdati (2006) analyzed the performance skyhook, groundhook, and hybrid control algorithm. Sohn *et al*. (2000) further proposed an improved version of skyhook control method, namely skyhook linear approximation damper (SH-L) control. The SH-L method can handle variable damping, either with discrete damping coefficients, or with continuously variable damper (e.g., MR damper). Other control strategies including PI control (Wang *et al*. 2003), H∞ control (Choi *et al*. 2002), sliding mode control (Yagiz and Sakman 2005), fuzzy control (Eslaminasab *et al*. 2007, Sung *et al*. 2007); neural network control (Guo *et al*. 2004), have also been explored for semi-active suspensions. Besides, the applications of MR

*Corresponding author, Associate Professor
E-mail: sx@upc.edu.cn

http://www.techno-press.com/journals/sss&subpage=7
ISSN: 1738-1584 (Print), 1738-1991 (Online)

dampers were also investigated for high-speed trains (Chen *et al*. 2015, Ni *et al*. 2016). Due to its intrinsic restraint, the control forces in semi-active suspension are clipped. For example, semi-active MR damper can only provide control forces in the opposite direction of damper velocity, and thus its performances are still not as good as active controllers.

In previous studies, active dampers (e.g., ideal skyhook damper and LQR controller), may produce a damper force–displacement relationship with obvious negative stiffness feature that benefits vibration control performance (Iemura and Pradono 2005). Inspired by these observations, the vibration control performances of negative stiffness have been studied for different mechanical and civil structures, including isolation tables (Platus and Ferry 2007, Yang 2013), vehicle seats (Lee *et al*. 2007, Le and Ahn 2011), adjustable constant force systems (Liu *et al*. 2016), tunable stiffness systems (Churchill *et al*. 2016), stay cables (Li *et al*. 2008, Weber and Boston 2011, Shi *et al*. 2016, 2017a, b, Balch *et al*. 2017), cable-stayed bridges (Iemura and Pradono 2002), and buildings (Asai *et al*. 2013, Iemura *et al*. 2006, Iemura and Pradono 2009, Pasala *et al*. 2012, Sun *et al*. 2017). Particularly, the feasibility of applying the negative stiffness in high-speed train suspensions has also been investigated (Lee and Goverdovskiy 2012, Lee *et al*. 2016, Shi *et al*. 2018). Numerical investigations verify that the re-centering negative stiffness damper can improve the ride comfort of high-speed trains without amplifying spring deflection (Shi *et al*. 2018). However, the performance analysis of negative stiffness on vehicle suspensions has not been conducted.

This work examines the benefits of negative stiffness in vibration control for vehicle suspensions. A re-centering negative stiffness device (NSD) is proposed to work in parallel with passive and semi-active suspension systems. The re-centering NSD consists of a passive magnetic negative stiffness spring and a positioning shaft with a re-centering function. The former produces negative stiffness control forces, and the latter prevents the amplification of static spring deflection. A common quarter-car suspension model was built, and both passive and semi-active suspensions were considered. With respect to ride comfort and road holding of a vehicle, the influence of negative stiffness on the performances of various vehicle suspension systems were analyzed.

2. Negative stiffness

Negative stiffness exhibits a negative slope in the force-deformation relationship (Fig. 1). In contrast with common positive stiffness, negative stiffness implies that the instantaneous direction of the external force is opposite to that of the deformation. To realize passive negative stiffness, several means have been developed, including: a pre-buckled beam with a snap-through behavior (Wang and Lakes 2004, Lee *et al*. 2007), a pre-compressed spring producing negative stiffness behavior in lateral direction (Pasala 2012), a friction pendulum isolator sliding on a convex friction interface (Iemura and Pradono 2009), and magnetic negative stiffness integrated with eddy-current damping (Shi and Zhu 2015, 2017).

Fig. 2 shows the conceptual design of the re-centering NSD for vehicle suspensions. The re-centering NSD is composed of a passive magnetic negative stiffness and a re-positioning shaft (Fig. 2). Magnetic negative stiffness is used to produce the negative stiffness force, and the re-centering shaft is used to avoid large spring deflection by re-centering the zero-displacement location of negative stiffness.

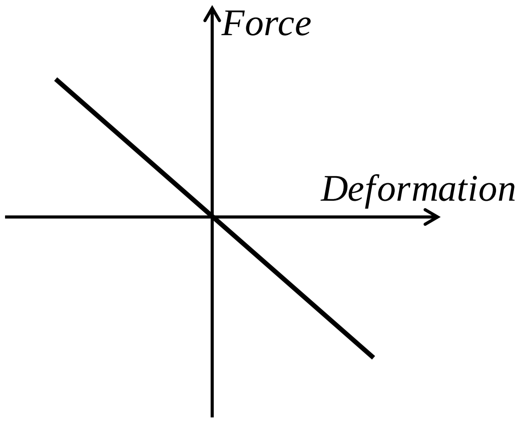

(a) Negative stiffness

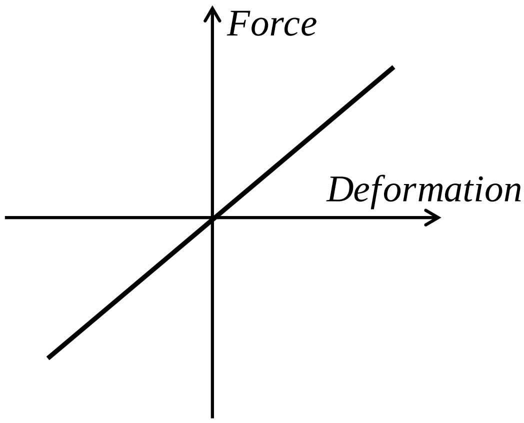

(b) Positive stiffness

Fig. 1 Force vs. deformation relationship

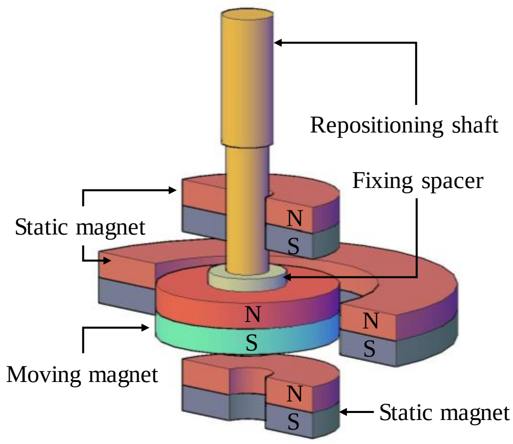

Fig. 2 Principle design of re-centering NSD

2.1 Passive magnetic negative stiffness

The magnetic negative stiffness consists of moving magnet and static magnets with the same pole orientation. The design is the combination of the two designs proposed by Shi and Zhu (2015), namely MNSD-A and MNSD-B. The corresponding design and optimization methods were also developed (Shi and Zhu 2017). According to the experimental results shown in Fig. 3 (Shi and Zhu 2015, 2017), the negative stiffness of MNSD-A can achieve -5000 N/m (three NdFeB magnets, grade N48, outer radius 24mm, inner radius 5 mm, thickness 20 mm), and the negative stiffness of MNSD-B can achieve -15000 N/m (two NdFeB magnets, grade N35, outer radius of static magnet 38 mm, inner radius of static magnet 25 mm, thickness of static magnet 20 mm, outer radius of moving magnet 20 mm, inner radius of moving magnet 5 mm, thickness of moving magnet 20 mm).

The stiffness requirements of various applications can be satisfied by magnetic negative stiffness. The control forces of magnetic negative stiffness can be flexibly designed through magnet dimension, strength and arrangement.

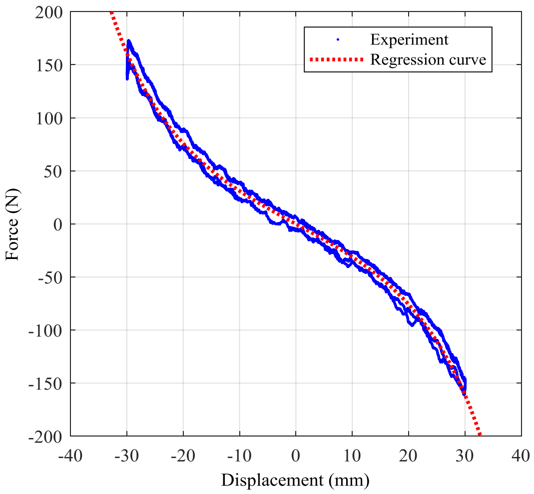

(a) Hardening

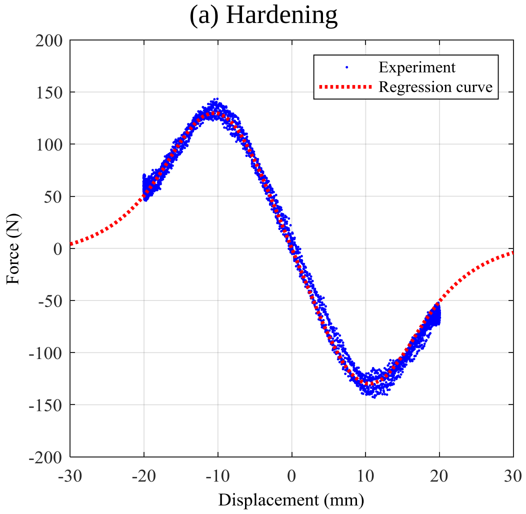

(b) Softening

Fig. 3 Negative stiffness behavior (Shi and Zhu 2015)

According to the principle design presented in Fig. 2, the interaction force between the moving magnet and the two static magnets at the ends nonlinearly increases with displacement at an increasing rate, which means the negative stiffness hardens with displacement; while interaction force between the moving magnet and the middle static magnet also increases with displacement but at a decreasing rate, which means the negative stiffness softens with displacement. Combine the hardening and softening stiffness properly, linear negative stiffness can also be achieved.

2.2 Re-centering function

Suspension systems not only need to isolate dynamic excitations, but also support the vehicle body. Simply reducing suspension stiffness will result in large static spring deflection. However, when the negative stiffness is installed in parallel with suspension stiffness, large static spring deflection can be avoided if the static loads are all supported by suspension stiffness, and negative stiffness only responds to dynamic excitations. This can be realized by locating the zero-displacement location of negative stiffness at the location of static load response. Since the static load from vehicle body may change, for example, different number of passengers or cargo weight, re-centering function is needed to accommodate the static load change.

The principle of the re-centering function is presented in Fig. 4. The static load on a vehicle is measured by sensors. The corresponding suspension deflection change (Δx) can be calculated with respect to the original stiffness of vehicle suspension, and then the re-positioning shaft can change the same amount of its length. As a result, the zero-displacement location of negative stiffness always coincides with the static load response. Therefore, the static load is all carried by the original stiffness of the vehicle suspension, so that the spring deflection will not be amplified. In practice, actuators of the re-positioning shaft could be a linear motor, a rotary motor with a ball screw, or a rotary motor with pinion and rack.

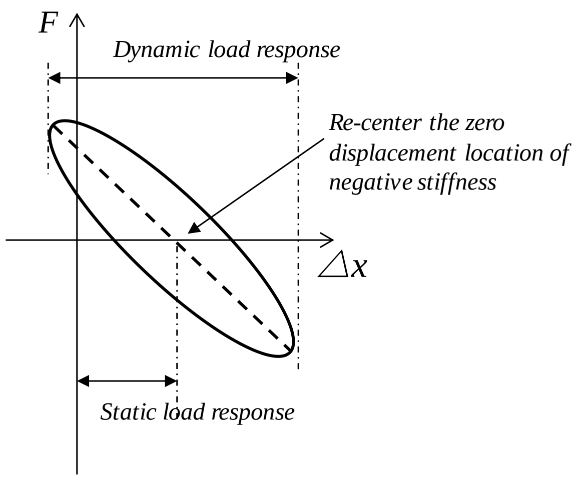

Fig. 4 Principle of re-centering function

Such a re-centering function belongs to low-bandwidth control because the changing rate of static load is very low. Similar low-bandwidth control has been implemented in vehicle suspensions, such as elevation control of vehicle through air springs. Through the re-centering function, the total stiffness of the suspension systems with negative stiffness is high for static load and low for dynamic excitation.

3. Dynamic formulation

3.1 Quarter-car suspension model

Quarter-car suspension models are widely adopted in literature for the simulation of real suspension systems. In this study, the quarter-car model was adopted to evaluate the performance of suspension systems. As shown in Fig. 5, the model includes one wheel, one-fourth of the car body mass and suspension components. The sprung mass m_s and unsprung mass m_u represent car chassis and wheel assembly, respectively; k_s and k_t are the stiffness of the uncontrolled suspension system and pneumatic tyre, respectively; The governing equations of the quarter-car suspension model are given by

$$m_s\ddot{z}_s + k_s\left(z_s - z_u\right) = -u \tag{1}$$

$$m_u\ddot{z}_u + k_s\left(z_u - z_s\right) + k_t\left(z_u - z_r\right) = u \tag{2}$$

where z_s and z_u are the displacement of the sprung and unsprung masses, respectively; z_r is the road displacement input; u is the control forces, which are produced by passive or semi-active dampers.

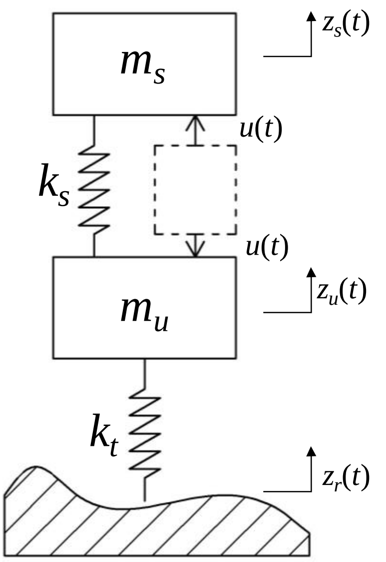

Fig. 5 Quarter-car suspension model

Ride comfort and road holding are the main performance criteria for vehicle suspension systems. Ride comfort is dependent on the acceleration of the sprung mass, while road holding is described by the tyre deflection. The new state variables are defined as

$$\begin{aligned} x_1(t) &= z_s(t) - z_u(t), \\ x_2(t) &= z_u(t) - z_r(t), \\ x_3(t) &= \dot{z}_s(t), \\ x_4(t) &= \dot{z}_u(t) \end{aligned} \tag{3}$$

where $x_1(t)$ is the suspension deflection, $x_2(t)$ is the tyre deflection, $x_3(t)$ is the sprung mass vibration speed, $x_4(t)$ is the unsprung mass vibration speed.

Eqs. (1) and (2) can be written in state-space form as

$$\dot{\mathbf{x}} = \mathbf{Ax} + \mathbf{B_c u} + \mathbf{B_w w} \tag{4}$$

where **x** is the state vector

$$\mathbf{x}(t) = \begin{bmatrix} x_1(t) & x_2(t) & x_3(t) & x_4(t) \end{bmatrix}^{\mathrm{T}} \tag{5}$$

u is the control force vector

$$\mathbf{u}(t) = u(t) \tag{6}$$

w is the vector representing the disturbance caused by road roughness

$$\mathbf{w}(t) = \dot{z}_r(t) \tag{7}$$

A is the state matrix

$$\mathbf{A} = \begin{bmatrix} 0 & 0 & 1 & -1 \\ 0 & 0 & 0 & 1 \\ -k_s/m_s & 0 & 0 & 0 \\ k_s/m_u & -k_t/m_u & 0 & 0 \end{bmatrix} \tag{8}$$

$\mathbf{B_w}$ is the input matrix for road roughness

$$\mathbf{B_w} = \begin{bmatrix} 0 & -1 & 0 & 0 \end{bmatrix}^{\mathrm{T}} \tag{9}$$

and $\mathbf{B_c}$ is the input matrix for the control forces

$$\mathbf{B}_c = \begin{bmatrix} 0 & 0 & -1/\mathrm{m_s} & 1/m_u \end{bmatrix}^T \tag{10}$$

On the basis of the quarter-car model, four representative suspension systems S1 to S4 are developed. Fig. 6 presents the four suspension systems analyzed in this paper. Suspension S1 models passive damper; S2 models negative stiffness and passive damper installed in parallel; S3 models semi-active damper, S4 models negative stiffness and semi-active damper installed in parallel. The mathematical models of the four suspension systems S1-S4 are formulated in following sections.

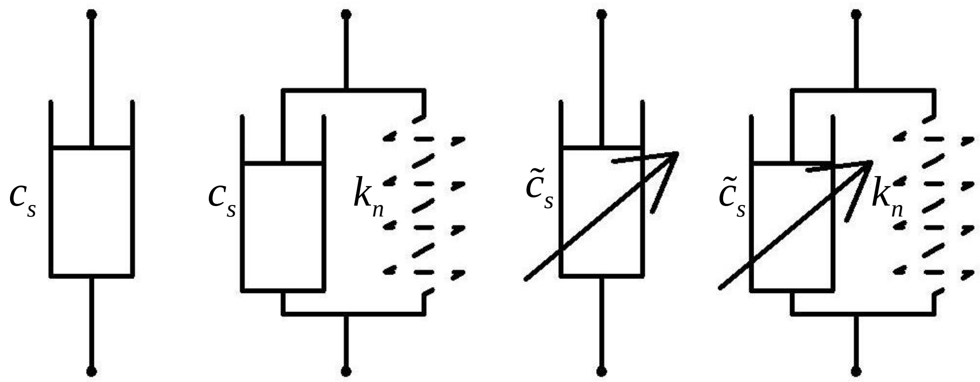

(a) S1 (b) S2 (c) S3 (d) S4

Fig. 6 Passive and semi-active suspension systems

3.2 Passive suspension

The control force u_1 of the passive suspension system S1 can be calculated by

$$u_1(t) = c_s \dot{x}_1(t) \tag{11}$$

where c_s is the damping coefficient for suspension S1.

After negative stiffness is installed, the control force u_2 of suspension system S2 shall be revised as

$$u_2(t) = -k_n x_1(t) + c_s \dot{x}_1(t) \tag{12}$$

where k_n is the stiffness value of negative stiffness. The negative sign in front of k_n indicates that the stiffness is negative.

The design of passive suspensions focuses on optimizing parameters of the suspension systems. Based on H2-norm performance measures, Scheibe and Smith (2009) have derived analytical solutions for the optima of ride comfort and road holding for a quarter-car vehicle model.

With respect to ride comfort, for fixed m_s, m_u, k_t and k_s, there exists an optimal damping coefficient (Scheibe and Smith 2009)

$$c_{opt1} = \sqrt{\frac{(m_u + m_s)}{k_t}} \cdot k_s \tag{13}$$

with

$$\min_{c \geq 0} H_1 = \frac{\sqrt{k_t (m_u + m_s)}}{m_s^2} \cdot k_s \tag{14}$$

where H_1 is the H_2-norm performance measure index for ride comfort.

With respect to road holding, for fixed m_s, m_u, k_t and k_s, there also exist an optimal damping coefficient (Scheibe and Smith 2009)

$$c_{opt2} = \sqrt{\frac{a_2}{a_1}} \tag{15}$$

with

$$\min_{c \geq 0} H_2 = 2\sqrt{a_1 a_2} \tag{16}$$

where H_2 is the H_2-norm performance measure index for road holding, and

$$\begin{aligned} a_1 &= \frac{(m_u + m_s)^2 k_t}{2m_s^2} \\ a_2 &= \frac{(m_u + m_s)^3 k_s^2 - 2m_u m_s (m_u + m_s) k_s k_t + m_u (m_s k_t)^2}{2m_s^2} \end{aligned} \tag{17}$$

3.3 Semi-active suspension

The control force u_3 of the semi-active suspension system S3 can be calculated by

$$u_3(t) = \tilde{c}_s \dot{x}_1(t) \tag{18}$$

where $\tilde{c}_s$ is the variable damping coefficient for suspension S3.

After negative stiffness is installed, the control force u_4 of suspension system S4 shall be revised as

$$u_4(t) = -k_n x_1(t) + \tilde{c}_s \dot{x}_1(t) \tag{19}$$

The SH-L control algorithm is employed for the semi-active suspension S3 and S4. Mathematically, the variable damping coefficient of SH-L can be described by (Sohn *et al*. 2000)

$$\tilde{c}_s = \begin{cases} c_{\min}, \text{ if } \dot{x}_1 x_3 \leq 0 \\ \mathbf{sat}_{\tilde{c} \in [c_{\min}; c_{\max}]} \left(\frac{\alpha c_{\max} \dot{x}_1 + (1-\alpha) c_{\max} x_3}{\dot{x}_1} \right), \text{ if } \dot{x}_1 x_3 > 0 \end{cases} \tag{20}$$

where $c_{\min}$ and $c_{\max}$ are the minimal and maximal damping coefficients achievable by the controlled damper respectively. $\alpha \in [0, 1]$ is a tuning parameter that modifies the closed-loop performances. When $\alpha = 0$, SH-L is equivalent to the two-states Skyhook control.

3.4 Road excitation

According to ISO standard ISO/TC108 and the Chinese standard GB7031-86, the power spectral density of road roughness can be described by

$$G_{z_r}(n) = G_{z_r}(n_0)\left(\frac{n}{n_0}\right)^{-W} \tag{21}$$

where n is spatial frequency, n_0 = 0.1 m^{-1} is the reference spatial frequency, $G_{z_r}(n_0)$ is the reference power spectral density at n_0, W=2 is the frequency attenuation index. Table 1 summarizes the classification of road roughness, and Fig. 7 presents the road surface profile and its PSD of a level C road.

If a vehicle travels at a speed of V, then the spatial power spectrum can be transferred into time power spectrum

$$G_{z_r}(f) = \frac{1}{V} G_{z_r}(n) \tag{22}$$

where $f = Vn$ is the frequency.

Based on Eq. (22), the velocity power spectrum for road roughness is

$$G_{\dot{z}_r}(f) = (2\pi f)^2 G_{z_r}(n) = 4\pi^2 G_{z_r}(n_0) n_0^2 V \tag{23}$$

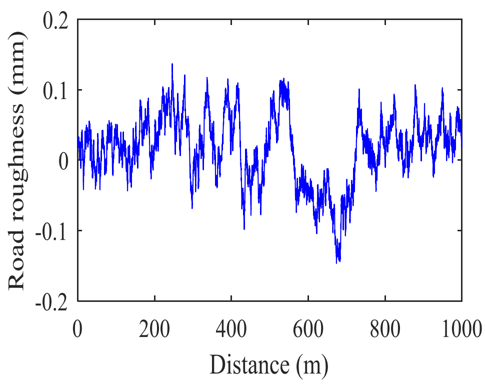

(a) Road surface profile

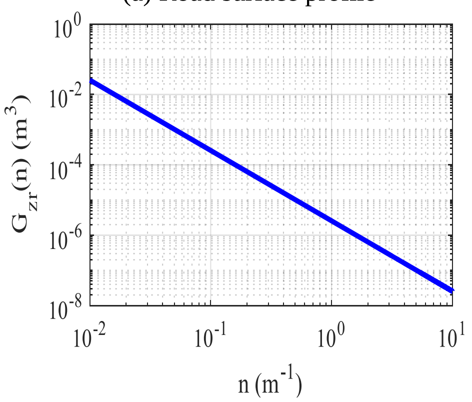

(b) PSD

Fig. 7 Road roughness of Level C road

Table 1 Classification on road roughness (GB7031-86)

Road level	$G_{z_r}(n_0)$ 10^{-6}m^3 (n_0=0.1m^{-1})
A	16
B	64
C	256
D	1024
E	4096
F	16384
G	65536
H	262144

According to Eq. (23), the $G_{\dot{z}_r}(f)$ is constant at different frequencies which is white noise, and its amplitude is only related with $G_{z_r}(n_0)$ and vehicle speed V.

4. Performance evaluation

In this section, the dynamic responses of the quarter-car model with suspension systems S1-S4 are simulated. The values of the quarter-car suspension model parameters are presented in Table 2. The simulation results are presented form Fig. 8 to Fig. 13 In those figures, the blue solid lines and red dashed lines present the results without and with negative stiffness installed, respectively.

4.1 Passive suspension

In design of passive vehicle suspension, there exists a trade-off between ride comfort and road holding performances. According to Table 2, for comfort-oriented purpose, the optimal damping coefficient is 621 Ns/m; while for control-oriented purpose, the damping coefficient is 3366 Ns/m. The performance influences of negative stiffness are analyzed for both comfort- and control-oriented passive suspensions, separately. In the analysis, the negative stiffness $k_n = 0.6k_s$.

Figs. 8 and 9 present the time histories and frequency domain responses of the quarter-car model with passive suspension (comfort-oriented), respectively. The tyre deflections in time and frequency domain are presented by Figs. 8(a) and 9(a), respectively.

Table 2 Quarter-car suspension model parameters (Du *et al*. 2005)

Parameters	Value
m_s	504.5 kg
m_u	62 kg
k_s	13100 N/m
k_t	252000 N/m

According to Fig. 8(a), the root-mean-square (RMS) of tyre deflections are 1.952 mm and 1.998 mm for suspension S1 and S2, respectively. Negative stiffness has very limited impact on the tyre deflection for passive suspension (comfort-oriented). In frequency domain, the resonant peak at high frequency are not affected by negative stiffness; while at low resonant frequency, both the amplitude and resonant frequency are reduced by negative stiffness (Fig. 9(a)). The sprung mass accelerations in time and frequency domain are shown in Figs. 8(b) and 9(b), respectively. The RMSs of sprung mass accelerations are 226.3 mm/s^2 and 171.5 mm/s^2 for suspension S1 and S2, respectively (Fig 8(b)). After installation of negative stiffness, the RMS of sprung mass acceleration is reduced by 24%. Similar with tyre defection, negative stiffness is effective for reducing the responses around low resonant frequency, but has limited impact on the responses around high resonant frequency (Fig. 9(b)).

Figs. 10 and 11 present the time histories and frequency domain responses of the quarter-car model with passive suspension (control-oriented), respectively. The tyre deflections in time and frequency domain are presented by Figs. 10(a) and 11(a), respectively.

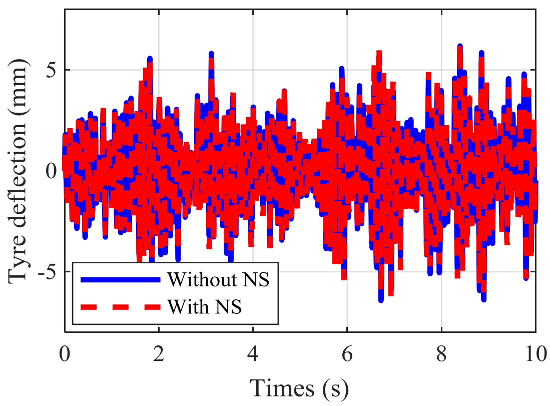

(a) Tyre deflection

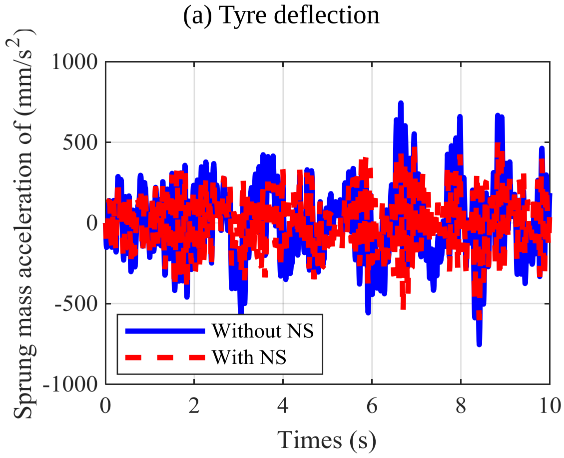

(b) Sprung mass accelerations

Fig. 8 Time history of quarter-car model responses with passive suspension (comfort-oriented)

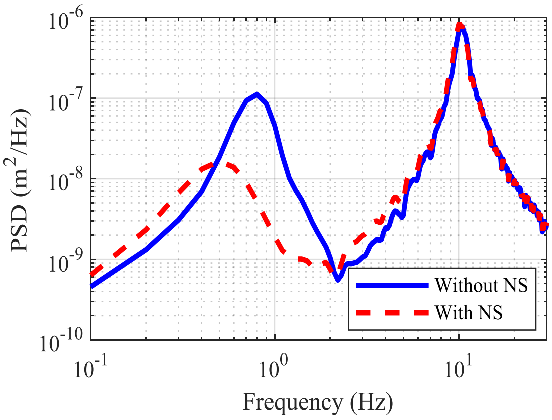

(a) Tyre deflection

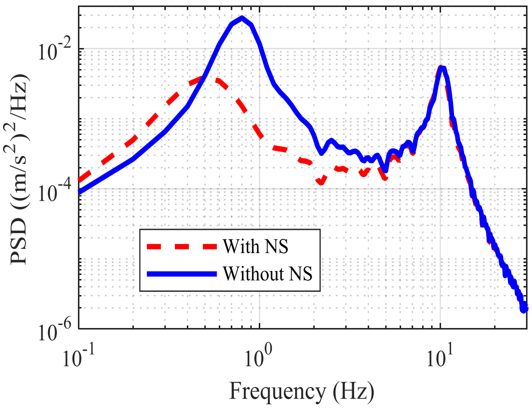

(b) Sprung mass accelerations

Fig. 9 PSD of quarter-car model responses with passive suspension (comfort-oriented)

According to Fig. 10(a), the RMSs of tyre deflections are 1.140 mm and 1.155 mm for suspension S1 and S2, respectively. Compared with the RMSs of comfort-oriented suspensions, the tyre deflections are much lower, but the impact from negative stiffness is still very limited. In frequency domain, the resonant peak at high frequencies are not affected by negative stiffness; while at low resonant frequency, the amplitude and resonant frequency are also reduced by negative stiffness (Fig. 11(a)), but the reduced degree is smaller than that of comfort-oriented passive suspension (Fig. 9(a)). The sprung mass accelerations in time and frequency domain are shown in Figs. 10(b) and 11(b), respectively. The RMSs of sprung mass accelerations are 377.5 mm/s^2 and 372.2 mm/s^2 for suspension S1 and S2. Respectively (Fig. 10(b)). Compared with the comfort-oriented suspension, the accelerations of sprung mass are much larger, and negative stiffness becomes ineffective (Figs. 8(b) and 10(b)). In frequency domain, negative stiffness can only reduce the responses around low resonant frequency by a less amount, compared with the comfort-orientation designed case (Figs. 9(b) and 11(b)).

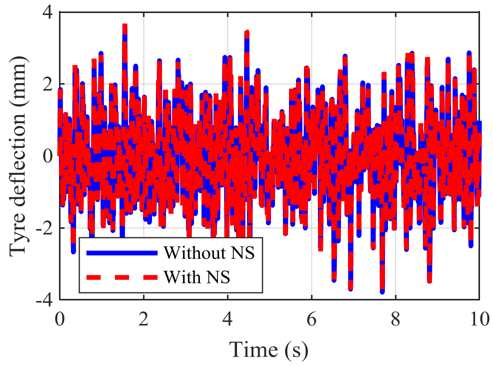

(a) Tyre deflection

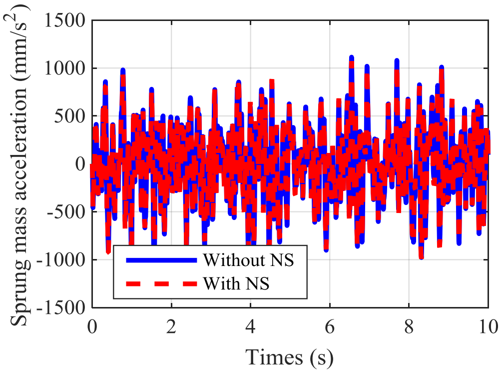

(b) Sprung mass accelerations

Fig. 10 Time history of quarter-car model responses with passive suspension (control-oriented)

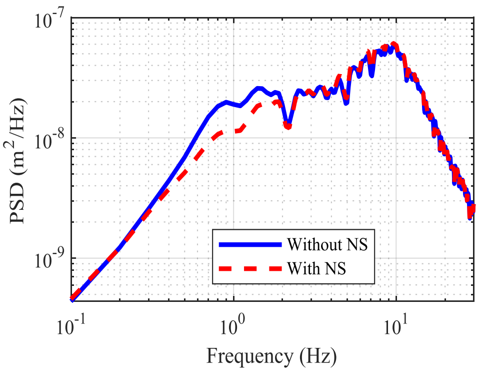

(a) Tyre deflection

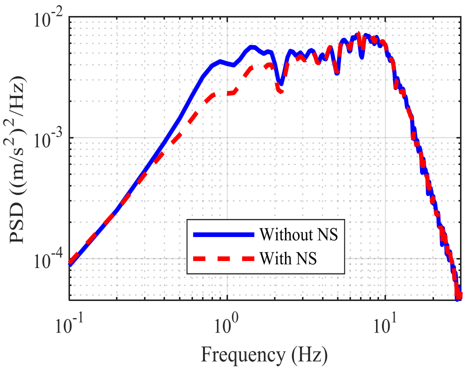

(b) Sprung mass accelerations

Fig. 11 PSD of quarter-car model responses with passive suspension (control-oriented)

4.2 Semi-active suspension

The semi-active suspension systems S3 and S4 employ the SH-L control algorithm. The α is set to be 0.5, and the minimal and maximal damping coefficients are 621 Ns/m and 3366 Ns/m, respectively. In suspension system S4, the negative stiffness k_n = -0.6k_s. Figs. 12 and 13 present the time histories and frequency domain responses of the quarter-car model with semi-active suspension systems, respectively.

The tyre deflections in time and frequency domain are presented by Figs. 12(a) and 13(a), respectively. According to Fig. 12(a), the RMS of tyre deflections are 1.122 mm and 1.245 mm for suspension S3 and S4, respectively. Same as in passive suspensions, negative stiffness has very limited impact on the tyre deflection in semi-active suspension. Compared with passive suspensions (Figs. 9(a) and 11(a)), semi-active suspension is more effect for reducing the low frequency vibrations in tyre deflection (Fig. 13(a)). Installation of negative stiffness can further reduce the vibration in low frequency range, but still ineffective at high frequencies (Fig. 13(a)).

The sprung mass accelerations in time and frequency domain are shown in Figs. 12(b) and 13(b), respectively. The RMS of sprung mass accelerations are 230.3 mm/s^2 and 218.2 mm/s^2 for suspension S3 and S4, respectively (Figs. 12(b)). Same as in passive suspensions, negative stiffness can reduce the sprung mass accelerations.

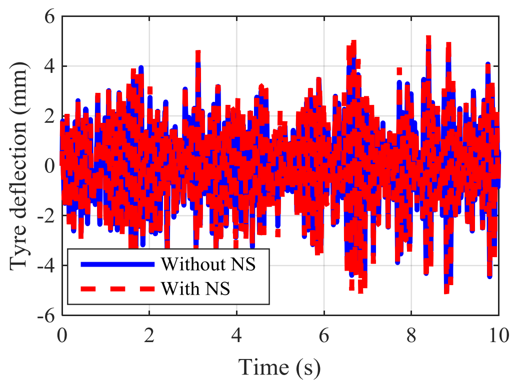

(a) Tyre deflection

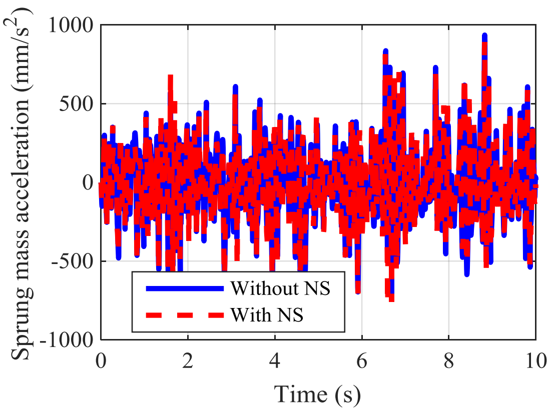

(b) Sprung mass accelerations

Fig. 12 Time history of quarter-car model responses with semi-active suspension

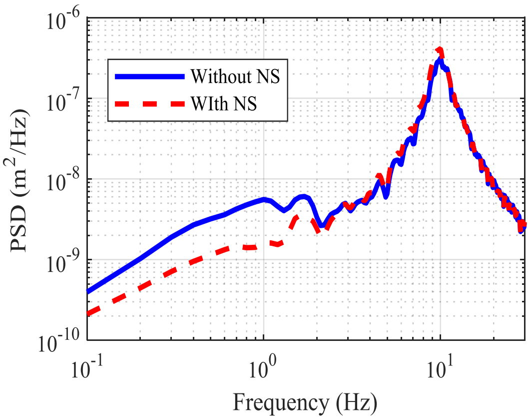

(a) Tyre deflection

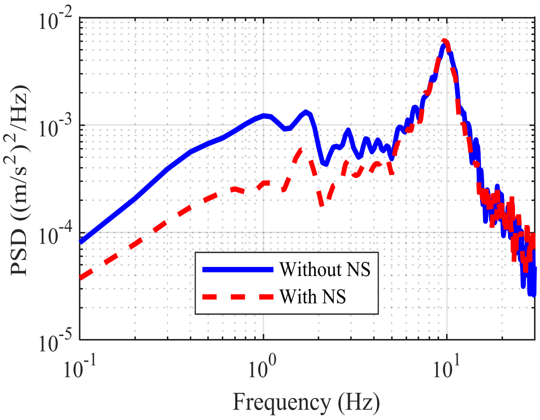

(b) Sprung mass accelerations

Fig. 13 PSD of quarter-car model responses with semi-active suspension

Table 3 RMS of sprung mass acceleration under various suspension systems

k_n (N/m)	Sprung mass acceleration (mm/s^2)		
	Passive suspension (control-oriented design)	Passive suspension (comfort-oriented design)	Semi-active suspension
0	377.498	226.327	230.264
1310	376.307	215.632	227.856
2620	375.237	205.443	225.921
3930	374.290	195.450	224.039
5240	373.468	185.422	222.303
6550	372.771	177.327	220.316
7860	372.199	171.507	218.166
9170	371.753	166.663	217.142
10480	371.432	162.899	215.400
11790	371.237	160.540	213.136

Table 4 RMS of tyre deflection under various suspension systems

k_n (N/m)	Tyre deflection (mm)		
	Passive suspension (control-oriented design)	Passive suspension (comfort-oriented design)	Semi-active suspension
0	1.140	1.952	1.541
1310	1.142	1.958	1.561
2620	1.144	1.965	1.583
3930	1.146	1.973	1.602
5240	1.149	1.980	1.626
6550	1.152	1.989	1.652
7860	1.155	1.998	1.679
9170	1.158	2.008	1.715
10480	1.161	2.019	1.757
11790	1.165	2.030	1.794

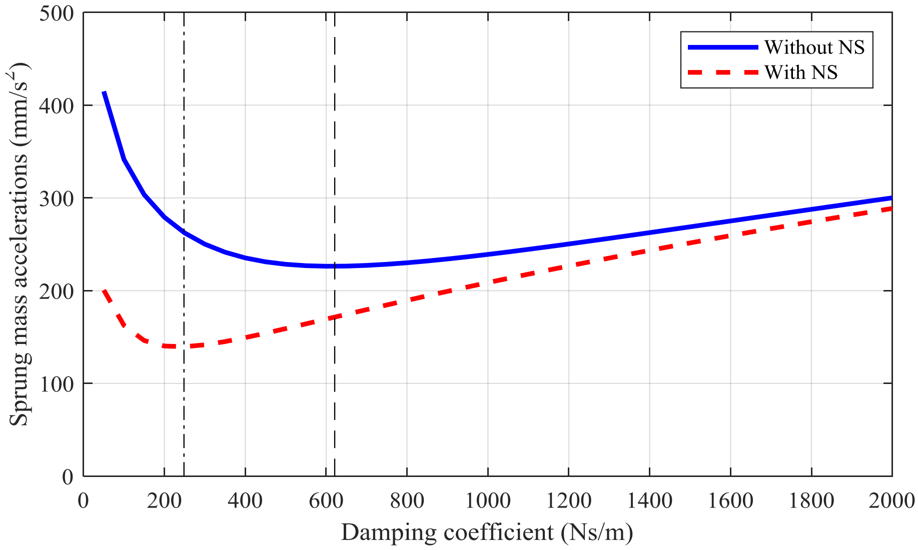

Fig. 14 RMS of sprung mass acceleration vs. damping coefficient of passive suspension

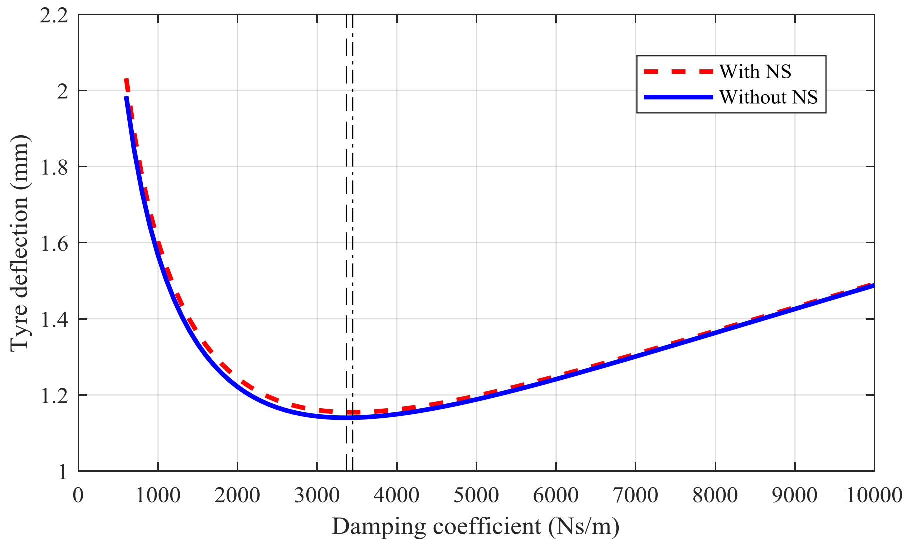

Fig. 15 RMS of tyre deflection vs. damping coefficient of passive suspension

The reduce degree in sprung mass accelerations of semi-active suspension (Fig. 13(b)) is larger than the degree of passive suspensions designed with control-orientation (Fig. 11(b)), but smaller than the degree of passive suspensions designed with comfort-orientation (Fig. 9(b)). Same conclusions can be drawn from the frequency domain responses. The responses of sprung mass at low frequencies are visibly reduced by negative stiffness (Fig. 13(b)).

In summary, negative stiffness can improve the ride comfort of a vehicle without affecting its road holding performances, for both passive and semi-active suspension systems. Comparing among the different suspension systems, the improvement in ride comfort from negative stiffness is related with damping coefficients adopted. In general, the improvement degree decreases, as the damping coefficient in passive suspension increases.

5. Performance analysis

5.1 Parametric analysis

The performance impact from negative stiffness is determined by negative stiffness itself and damping coefficients in suspension systems. Tables 3 and 4 summarize the RMS of sprung mass accelerations and tyre deflections with respect to negative stiffness, respectively. As the absolute negative stiffness value k_n increases from 0 N/m to 11790 N/m, the RMSs of sprung mass acceleration decreased from 377.5m/s^2 to 371.2 m/s^2 for control-oriented passive suspension; from 226.3m/s^2 to 160.5 m/s^2 for comfort-oriented passive suspension; and from 230.2m/s^2 to 213.1m/s^2 for semi-active suspension (Table 4). To improve ride comfort, negative stiffness is effective for comfort-oriented passive suspension and semi-active suspension

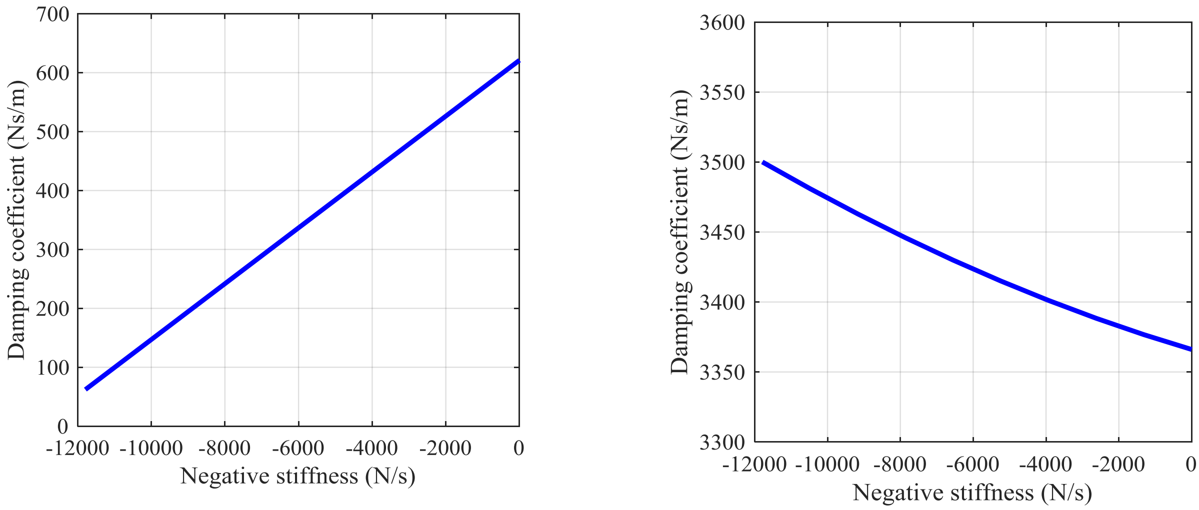

(a) Comfort-oriented (b) Control-oriented

Fig. 16 Optimal damping coefficient for passive suspension systems with negative stiffness

(most effective for comfort-oriented passive suspension), but ineffective for control-oriented passive suspension due to large damping coefficient. On the other hand, the tyre deflections are barely affected by negative stiffness, not matter for which types of suspension systems (Table 4).

Fig. 14 present the RMS of sprung mass accelerations vs. damping coefficients in passive suspensions. The blue solid line and red dashed line present the results without and with negative stiffness (k_n= $0.6k_s$) installed, respectively. After the installation of negative stiffness, both the sprung mass accelerations and the optimal damping coefficients are decreased (Fig. 14). For both with and without negative stiffness cases, there exists an optimal damping coefficient so that the sprung mass accelerations can be minimized (Fig. 14). Based on simulation results, the optimal damping coefficients for Without NS case and With NS case are 621 Ns/m and 248 Ns/m, respectively. These values also fit the analytical results calculated from Eq. (13).

Fig. 15 present the RMS of tyre deflections vs. damping coefficients in passive suspensions. The blue solid line and red dashed line present the results without and with negative stiffness (k_n= $0.6k_s$) installed, respectively. The impacts from negative stiffness are quite limited (Fig. 15). Based on simulation results, the optimal damping coefficients for Without NS case and With NS case are 3366 Ns/m and 3446 Ns/m, respectively. These values also fit the analytical results calculated from Eq. (15).

Fig. 16 present the variation of optimal damping coefficient with respect to negative stiffness. The optimal damping coefficients for comfort purpose decreases as negative stiffness becomes stronger (Fig. 16(a)); while the coefficients for control purpose increases as negative stiffness becomes stronger (Fig. 16(b)). It was also found that the variational extent of optimal damping coefficients for comfort purpose is much large than the extent for control purposes.

5.2 Damping force

Based on previous analysis, the influences of negative stiffness are different for passive and semi-active suspension systems. To explain this phenomenon, the control forces of comfort-oriented passive suspension, control-oriented passive suspension and semi-active suspension are plotted in Fig. 17, Figs. 18 and 19, respectively. For viscous damper (without negative stiffness), the plotted dots of force vs. suspension deflection forms ellipse (Figs. 17(a) and 18(a)); after negative stiffness is installed, the ellipse rotates. For a small damping coefficient adopted in comfort-oriented passive suspension, the rotation is obvious and a clear negative slope can be observed (Fig. 17(b)). For a large damping coefficient adopted in control-oriented passive suspension, the rotation is unobvious, so the influence of negative stiffness is limited (Fig. 18(b)). In general, the negative stiffness feature in control forces is beneficial for the ride comfort of vehicles.

The damping forces of semi-active suspension already possess negative stiffness feature, before installation of negative stiffness (Fig. 19(a)). However, due to the intrinsic restraint of semi-active suspension, the damping forces in same direction with damper vibration velocities cannot be produced. In SH-L algorithm (Eq. (20)), when the direction of relative velocity between sprung and unsprung masses is opposite to that of the sprung vibration velocity, the variable damping coefficients equals to its minimum. The clipped damping will result in sudden changes in damping forces. As marked by the dashed lines in Fig. 19(a), gaps can be found near the x-axis in the second and fourth quadrant. Those gaps are harmful for the ride comfort. Comparing Figs. 19(a) and 19(b), installation of negative stiffness can shrink the gap in the control forces of semi-active suspension. In other words, negative stiffness can alleviate the impact of clipped damping in semi-active suspension, and benefits the ride comfort of vehicles.

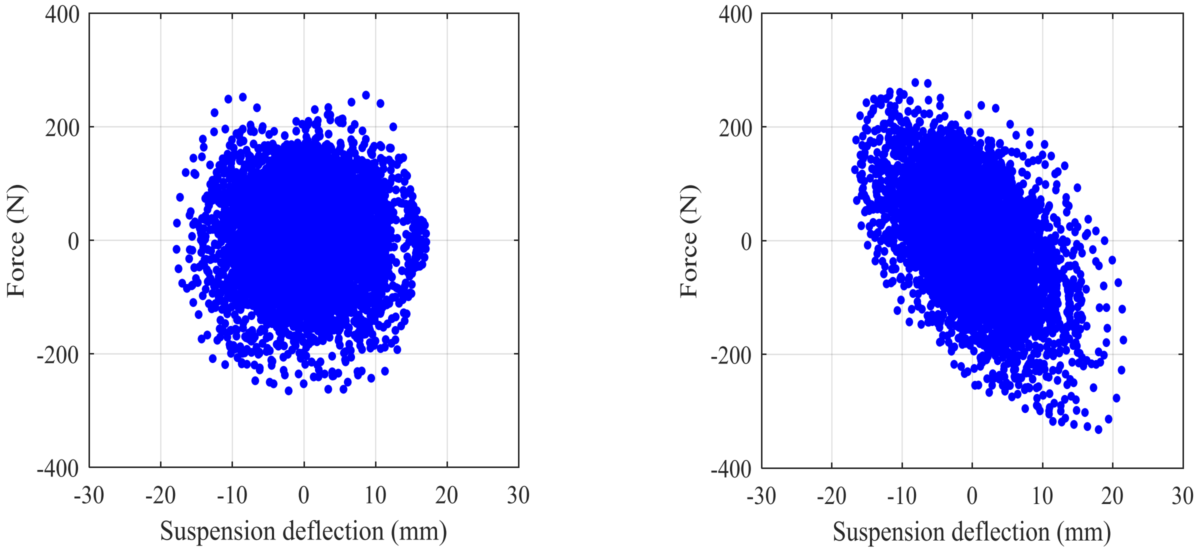

(a) Without negative stiffness (b) With negative stiffness

Fig. 17 Force vs. suspension deflection of passive suspension (Comfort-oriented)

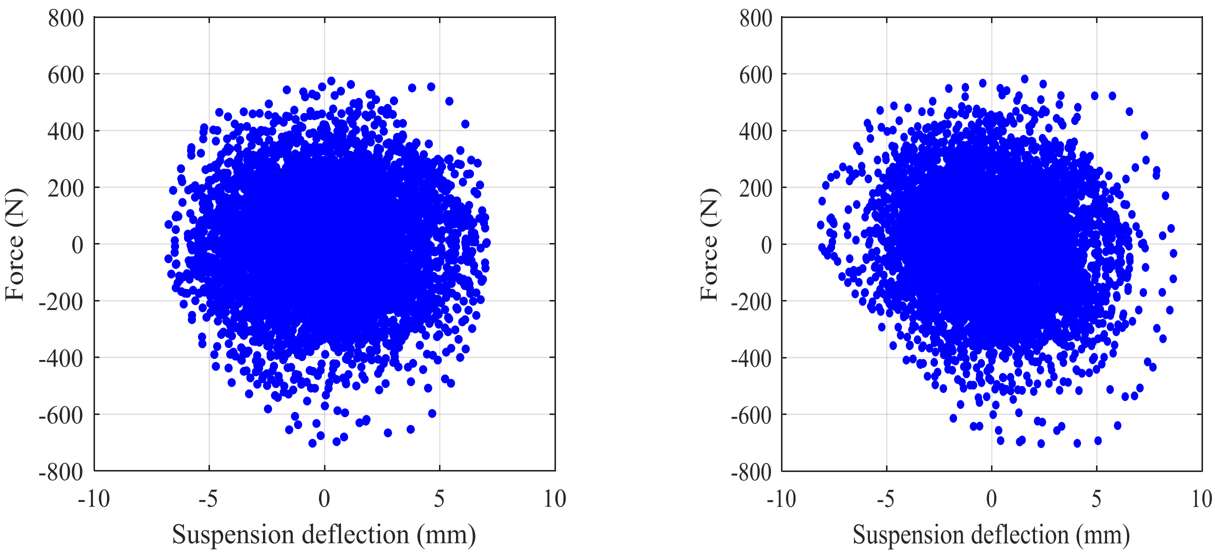

(a) Without negative stiffness (b) With negative stiffness

Fig. 18 Force vs. suspension deflection of passive suspension (Control-oriented)

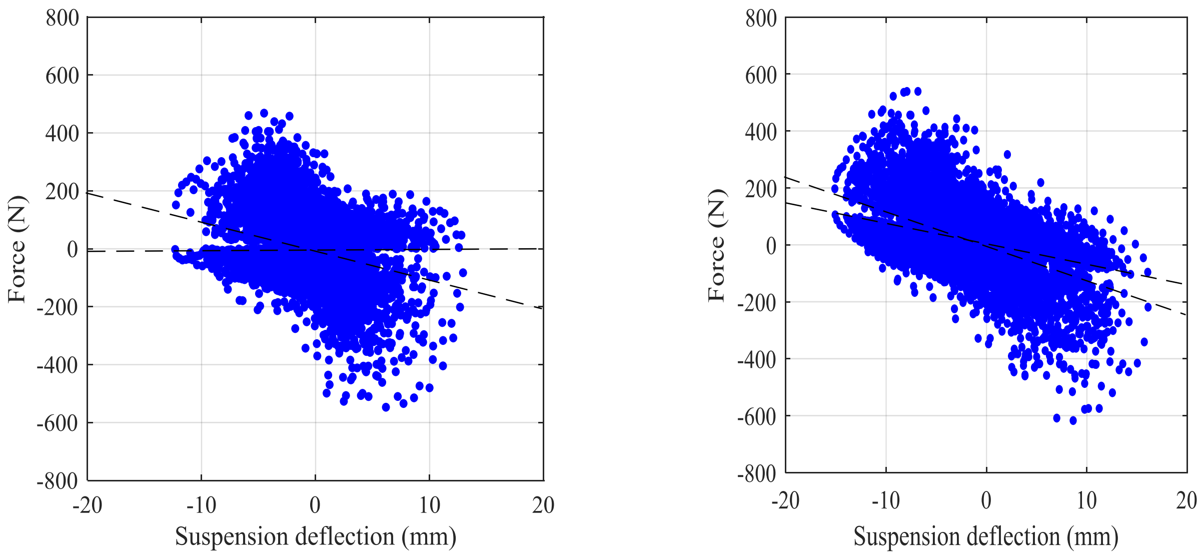

(a) Without negative stiffness (b) With negative stiffness

Fig. 19 Force vs. suspension deflection of semi-active suspension

6. Conclusions

This work evaluates the performance influence of negative stiffness on various vehicle suspension systems. A common quarter-car suspension model is built, and the comfort- and control- oriented passive suspensions and semi-active suspension employed with SH-L algorithm are analyzed. A re-centering NSD is proposed to work in parallel with passive and semi-active suspension systems. The re-centering NSD consists of a passive magnetic negative stiffness spring and a positioning shaft with a re-centering function. The former produces negative stiffness control forces, and the latter prevents the amplification of static spring deflection. The numerical simulations reveal that negative stiffness can improve the ride comfort of a vehicle without affecting its road holding performances, for both passive and semi-active suspension systems. For passive suspension system, negative stiffness brings in negative stiffness feature in control forces, which is helpful for the ride comfort of a vehicle. For semi-active suspensions, negative stiffness can alleviate the impact of clipped damping in semi-active damper, and benefits the ride comfort of vehicles.

Acknowledgments

The authors are grateful for the financial support from China University of Petroleum (East China) (Project No. Y18050010). The findings and opinions expressed in this paper are solely those of the authors and are not necessarily the views of sponsors.

References

Ahmadian, M. and Vahdati, N. (2006), “Transient dynamics of semiactive suspensions with hybrid control”, *J. Intel. Mat. Syst. Str.*, **17**(2), 145-153. https://doi.org/10.1177/1045389X06056458.

Al-Holou, N., Lahdhiri, T., Joo, D.S., Weaver, J. and Al-Abbas, F. (2002), “Sliding mode neural network inference fuzzy logic control for active suspension systems”, *IEEE T. Fuzzy Syst.*, **10**(2), 234-246. DOI: 10.1109/91.995124

Asai, T., Spencer, B.F., Iemura, H. and Chang, C.M. (2013), “Nature of seismic control force in acceleration feedback”, *Struct. Control Health Monit.*, **20**(5), 789-803. https://doi.org/10.1002/stc.1496.

Balch, S.P. and Lakes, R.S. (2017), “Lumped negative stiffness damper for absorption of flexural waves in a rod”, *Smart Mater. Struct.*, **26**(4), 045022.

Chen, Z. H., Ni, Y.Q. and Or, S.W. (2015), “Characterization and modeling of a self-sensing MR damper under harmonic loading”, *Smart Struct. Syst.*, **15**(4), 1103-1120. https://doi.org/10.12989/sss.2015.15.4.1103.

Choi, J.W., See, Y.B., Yoo, W.S. and Lee, M.H. (1998), “LQR approach using eigenstructure assignment with an active suspension control application”, *Proceedings of the 1998 IEEE International Conference on Control Applications (Cat. No. 98CH36104)*, IEEE, September.

Choi, S.B., Lee, H.S. and Park, Y.P. (2002), “H8 control performance of a full-vehicle suspension featuring magnetorheological dampers”, *Vehicle Syst. Dyn.*, **38**(5), 341-360.

Churchill, C.B., Shahan, D.W., Smith, S.P., Keefe, A.C. and McKnight, G.P. (2016), “Dynamically variable negative stiffness structures”, *Sci. Adv.*, **2**(2), e1500778. DOI: 10.1126/sciadv.1500778.

Dong, X.M., Yu, M., Liao, C.R. and Chen, W.M. (2010), “Comparative research on semi-active control strategies for magneto-rheological suspension”, *Nonlinear Dynam.*, **59**(3), 433-453.

Du, H., Sze, K.Y. and Lam, J. (2005), “Semi-active H∞ control of vehicle suspension with magneto-rheological dampers”, *J.*

Sound Vib., **283**(3-5), 981-996. https://doi.org/10.1016/j.jsv.2004.05.030.

Eslaminasab, N., Biglarbegian, M., Melek, W.W. and Golnaraghi, M.F. (2007), "A neural network based fuzzy control approach to improve ride comfort and road handling of heavy vehicles using semi-active dampers", *Int. J. Heavy Veh. Syst.*, **14**(2), 135-157. https://doi.org/10.1504/IJHVS.2007.013259.

Fialho, I. and Balas, G.J. (2002), "Road adaptive active suspension design using linear parameter-varying gain-scheduling", *Institute of Electrical and Electronic Engineers*.

GB/T7031-1986 (1987), *Vehicle vibration-describing method for road surface irregularity*, Beijing: Standards Press of China (in Chinese).

Guo, D.L., Hu, H.Y. and Yi, J.Q. (2004), "Neural network control for a semi-active vehicle suspension with a magnetorheological damper", *Modal Anal.*, **10**(3), 461-471. https://doi.org/10.1177/1077546304038968.

Iemura, H. and Pradono, M.H. (2002), "Passive and semi-active seismic response control of a cable-stayed bridge", *Struct. Control Health Monit.*, **9**(3), 189-204. https://doi.org/10.1002/stc.12.

Iemura, H. and Pradono, M.H. (2005), "Simple algorithm for semi-active seismic response control of cable-stayed bridges", *Earthq. Eng. Struct. D.*, **34**(4-5), 409-423. https://doi.org/10.1002/eqe.440.

Iemura, H. and Pradono, M.H. (2009), "Advances in the development of pseudo-negative-stiffness dampers for seismic response control", *Struct. Control Health Monit.*, **16**(7-8), 784-799. https://doi.org/10.1002/stc.345.

Iemura, H., Igarashi, A., Pradono, M.H. and Kalantari, A. (2006), "Negative stiffness friction damping for seismically isolated structures", *Struct. Control Health Monit.*, **13**(2-3), 775-791. https://doi.org/10.1002/stc.111.

Kanarachos, S., Dizqah, A.M., Chrysakis, G. and Fitzpatrick, M. E., (2018), "Optimal design of a quadratic parameter varying vehicle suspension system using contrast-based fruit fly optimization", *Appl. Soft Comput.*, **62**, 463-477. https://doi.org/10.1016/j.asoc.2017.11.005.

Karlsson, N., Dahleh, M. and Hrovat, D., (2001), "Nonlinear H∞ control of active suspensions", *Proceedings of the 2001 American Control Conference, (Cat. No. 01CH37148)*, IEEE.

Le, T.D. and Ahn, K.K. (2011), "A vibration isolation system in low frequency excitation region using negative stiffness structure for vehicle seat", *J. Sound Vib.*, **330**(26), 6311-6335. https://doi.org/10.1016/j.jsv.2011.07.039.

Lee, C.M. and Goverdovskiy, V.N. (2012), "A multi-stage high-speed railroad vibration isolation system with "negative" stiffness", *J. Sound Vib.*, **331**(4), 914-921. https://doi.org/10.1016/j.jsv.2011.09.014.

Lee, C.M., Goverdovskiy, V.N. and Temnikov, A.I. (2007), "Design of springs with "negative" stiffness to improve vehicle driver vibration isolation", *J. Sound Vib.*, **302**(4-5), 865-874. https://doi.org/10.1016/j.jsv.2006.12.024.

Lee, C.M., Goverdovskiy, V.N., Sim, C.S. and Lee, J.H. (2016), "Ride comfort of a high-speed train through the structural upgrade of a bogie suspension", *J. Sound Vib.*, **361**, 99-107. https://doi.org/10.1016/j.jsv.2015.07.019.

Li, H., Liu, M. and Ou, J. (2008), "Negative stiffness characteristics of active and semi-active control systems for stay cables", *Struct. Control Health Monit.*, **15**(2), 120-142. https://doi.org/10.1002/stc.200.

Liu, Y., Yu, D.P. and Yao, J. (2016), "Design of an adjustable cam based constant force mechanism", *Mechanism and Machine Theory*, **103**, 85-97. https://doi.org/10.1016/j.mechmachtheory.2016.04.014.

Ni, Y.Q., Ye, S.Q. and Song, S.D. (2016), "An experimental study on constructing MR secondary suspension for high-speed trains to improve lateral ride comfort", *Smart Struct. Syst.*, **18**(1), 53-74. https://doi.org/10.12989/sss.2016.18.1.053.

Pasala, D.T.R., Sarlis, A.A., Nagarajaiah, S., Reinhorn, A.M., Constantinou, M.C. and Taylor, D. (2012), "Adaptive negative stiffness: new structural modification approach for seismic protection", *J. Struct. Eng.*, **139**(7), 1112-1123. https://doi.org/10.1061/(ASCE)ST.1943-541X.0000615.

Platus, D.L. and Ferry, D.K. (2007), "Negative-stiffness vibration isolation improves reliability of nanoinstrumentation", *Laser Focus World*, **43**(10), 107.

Priyandoko, G., Mailah, M. and Jamaluddin, H. (2009), "Vehicle active suspension system using skyhook adaptive neuro active force control", *Mech. Syst. Signal Pr.*, **23**(3), 855-868. https://doi.org/10.1016/j.ymssp.2008.07.014.

Savaresi, S. M., Silani, E., Bittanti, S. and Porciani, N. (2003). "On performance evaluation methods and control strategies for semi-active suspension systems", *Proceedings of the 42nd IEEE International Conference on Decision and Control (IEEE Cat. No. 03CH37475)*, IEEE, December.

Scheibe, F. and Smith, M.C. (2009), "Analytical solutions for optimal ride comfort and tyre grip for passive vehicle suspensions", *Vehicle Syst. Dynam.*, **47**(10), 1229-1252. https://doi.org/10.1080/00423110802588323.

Shi, X. and Zhu, S. (2015), "Magnetic negative stiffness dampers", *Smart Mater. Struct.*, **24**(7), 072002.

Shi, X. and Zhu, S. (2017), "Simulation and optimization of magnetic negative stiffness dampers", *Sensor. Actuat. A: Phys.*, **259**, 14-33. https://doi.org/10.1016/j.sna.2017.03.026.

Shi, X., Zhu, S. and Nagarajaiah, S. (2017b), "Performance comparison between passive negative-stiffness dampers and active control in cable vibration mitigation", *J. Bridge Eng.*, **22**(9), 04017054. https://doi.org/10.1061/(ASCE)BE.1943-5592.0001088.

Shi, X., Zhu, S. and Spencer, Jr. B.F. (2017a), "Experimental study on passive negative stiffness damper for cable vibration mitigation", *J. Eng. Mech.*, **143**(9), 04017070. https://doi.org/10.1061/(ASCE)EM.1943-7889.0001289.

Shi, X., Zhu, S., Li, J.Y. and Spencer, Jr. B.F. (2016), "Dynamic behavior of stay cables with passive negative stiffness dampers", *Smart Mater. Struct.*, **25**(7), 075044.

Shi, X., Zhu, S., Niu, Y.Q. and Li, J. (2018), "Vibration suppression in high-speed trains with negative stiffness dampers", *Smart Struct. Syst.*, **21**(5), 653-668. https://doi.org/10.12989/sss.2018.21.5.653.

Sohn, H.C., Hong, K.S. and Hedrick, J.K. (2000), "Semi-active control of the Macpherson suspension system: hardware-in-the-loop simulations", *Proceedings of the 2000. IEEE International Conference on Control Applications. Conference Proceedings (Cat. No. 00CH37162)*, IEEE.

Sun, T., Lai, Z., Nagarajaiah, S. and Li, H.N. (2017), "Negative stiffness device for seismic protection of smart base isolated benchmark building", *Struct. Control Health Monit.*. **24**(11), https://doi.org/10.1002/stc.1968.

Sung, K.G., Han, Y.M., Lim, K.H. and Choi, S.B. (2007), "Discrete-time fuzzy sliding mode control for a vehicle suspension system featuring an electrorheological fluid damper", *Smart Mater. Struct.*, **16**(3), 798.

Wang, E.R., Ma, X.Q., Rakheja, S. and Su, C.Y. (2003), "Semi-active control of vehicle vibration with MR-dampers", *In Decision and Control, 2003. Proceedings of the 42nd IEEE Conference on IEEE*, December.

Wang, H.P., Mustafa, G.I. and Tian, Y. (2018), "Model-free fractional-order sliding mode control for an active vehicle suspension system", *Adv. Eng. Softw.*, **115**, 452-461. https://doi.org/10.1016/j.advengsoft.2017.11.001.

Wang, Y.C. and Lakes, R.S. (2004), "Stable extremely-high-damping discrete viscoelastic systems due to negative stiffness elements", *Appl. Phys. Lett.*, **84**(22), 4451-4453. https://doi.org/10.1063/1.1759064.

Weber, F. and Boston, C. (2011), "Clipped viscous damping with negative stiffness for semi-active cable damping", *Smart Mater. Struct.*, **20**(4), 045007.

Yagiz, N. and Sakman, L.E. (2005), "Robust sliding mode control of a full vehicle without suspension gap loss", *Modal Anal.*, **11**(11), 1357-1374. https://doi.org/10.1177/1077546305058268.

Yang, J., Xiong, Y.P. and Xing, J.T. (2013), "Dynamics and power flow behaviour of a nonlinear vibration isolation system with a negative stiffness mechanism", *J. Sound Vib.*, **332**(1), 167-183. https://doi.org/10.1016/j.jsv.2012.08.010.

Yao, G.Z., Yap, F.F., Chen, G., Li, W. and Yeo, S.H. (2002), "MR damper and its application for semi-active control of vehicle suspension system", *Mechatronics*, **12**(7), 963-973. https://doi.org/10.1016/S0957-4158(01)00032-0.

Ying, Z.G., Zhu, W.Q. and Soong, T.T. (2003), "A stochastic optimal semi-active control strategy for ER/MR dampers", *J. Sound Vib.*, **259**(1), 45-62. https://doi.org/10.1006/jsvi.2002.5136.